PAPER

Check for updates

Synthesis of insensitive, high-density energetic materials through molecular self-assembly†

Jinhao Zhang,[a] Jichuan Zhang,*[ab] Richard J. Staples, [iD][c] Jiaheng Zhang [iD] *[a] and Jean'ne M. Shreeve [iD] *[b]

Development of insensitive high-energy materials through a simple strategy is still a challenging issue. In this work, five insensitive high-energy materials, namely, TNPDO-ADNP (**1**), TNPDO-DNBT (**2**), TNPDO-55BT (**3**), TNPDO-DNABO (**4**), and TNPDO-BTO (**5**), were prepared by the reaction between TNPDO, a high-density insensitive base and five high-energy acids, namely, ADNP (4-amino-3,5-dinitro-1*H*-pyrazole), DNBT (3,3′-dinitro-5,5′-bis-1,2,4-triazole), 55BT (5,5′-bitetrazole), DNABO (2,2′-dinitramino-5,5′-bis-1H,1′*H*-oxa-3,4-diazole), and BTO (1H,1′*H*-5,5′-bitetrazole-1,1′-diol), through molecular self-assembly in an aqueous solution. All the new materials exhibited high density (>1.85 g cm^{-3}), acceptable decomposition temperature (>185 °C), high detonation performance (>8376 m s^{-1}, >27.80 GPa) and insensitivity (>40 J, >360 N). The detonation properties of **3** were higher than those of either of its corresponding precursors, and the density of **4** was 1.96 g cm^{-3}, with a detonation velocity and pressure of 8895 m s^{-1} and 33.32 GPa, respectively, which were comparable with those of RDX. The density of **5** was 1.87 g cm^{-3}, which was higher than those of either of its precursors. The advantages of simple preparation, insensitivity, acceptable thermal stability and excellent detonation properties make these five materials promising. Moreover, this work may pave the way to the simple preparation strategies for low sensitive or insensitive high-energy materials.

Introduction

Energetic materials play an irreplaceable role in defense and civilian industries. High safety and high energy have always been the theme for the continuous development of energetic materials.[1–3] However, numerous unexpected accidents suggest that high safety should be prioritized over high energy.[4,5] As sensitivity (impact and friction sensitivity) is the main evaluation standard for safe, low sensitive or insensitive high-energetic materials, it has gained increased attention.[6–9] In general, there are two strategies to decrease the sensitivity of energetic materials: forming salts and subtle molecular design.[10,11] Salts usually decrease the energy density because of the introduction of a cation with a high hydrogen content,[12–15] but a new molecular structure most often suffers from multistep unknown reactions and dangerous experiments, leading

[a]Sauvage Laboratory for Smart Materials, Harbin Institute of Technology, Shenzhen 518055, China. E-mail: zhangjiaheng@hit.edu.cn

[b]Department of Chemistry, University of Idaho, Moscow, Idaho 83844-2343, USA. E-mail: jichuanz@uidaho.edu; jshreeve@uidaho.edu

[c]Department of Chemistry, Michigan State University, East Lansing, MI 48824, USA

† Electronic supplementary information (ESI) available: Preparation method, samples' picture, XRD, single crystal information, ESP calculations, densities, computation and properties. CCDC 2271444–2271446. For ESI and crystallographic data in CIF or other electronic format see DOI: https://doi.org/10.1039/d4ta07871c

to high cost. Therefore, it is a challenge to synthesize low sensitive or insensitive high-energy materials by employing a simple strategy.

Molecular self-assembly, which depends on intermolecular interactions, such as hydrogen bonding, π–π stacking or halogen bonding, has demonstrated huge promises in various fields of chemical materials, such as in molecular recognition, medicine cocrystal, transportation of active pharmaceutical ingredients, and gas separation.[16–19] For example, PFC-1 (PFC = porous materials as defined by the Fujian Institute of Research on the Structure of Matter and the Chemical Abstract Service) and HOF–NF (HOF = hydrogen-bonded organic frameworks, NF = nitroformate, melaminium nitroformate 3,6,7-triamino-7H-[1,2,4]triazolo[4,3-b][1,2,4]triazole) have high stabilities owing to their ultra-robust hydrogen-bonded organic frameworks.[20,21] PFC-1 has been demonstrated to be an excellent drug carrier for synergetic chemo-photodynamic therapy with the merit of low cytotoxicity and high efficacy.[20] Through hydrogen bonding, the thermal stability of nitroformate was improved to 200 °C from around 120 °C in HOF–NF. Therefore, molecular self-assembly is an efficient strategy to enhance stability.[21]

Recently, we made a breakthrough through the self-assembly of TNPDO (2,4,6-triamino-5-nitropyrimidine-1,3-dioxide), a Lewis basic insensitive molecule, and TNBI (4,4′,5,5′-tetranitro-2,2′-bi-1*H*-imidazole), a Lewis acidic sensitive molecule, and developed an insensitive high-energy material (TNPDO-TNBI).[22]

5164 | *J. Mater. Chem. A*, 2025, **13**, 5164–5168

This journal is © The Royal Society of Chemistry 2025

Notably, TNPDO-TNBI exhibited higher density and higher thermal stability than either of its precursors. This work suggested that the strategy of self-assembly is promising in developing high-energy and low-sensitive or insensitive materials. In this work, benefiting from the high density and insensitivity of TNPDO,[23,24] five acidic high-energy molecules (ADNP: 4-amino-3,5-dinitro-1H-pyrazole; DNBT: 3,3′-dinitro-5,5′-bis-1,2,4-triazole; 55BT:5,5′-bitetrazole; DNABO: 2,2′-dinitramino-5,5′-bis-1H,1′H-oxa-3,4-diazole; and BTO: 1H,1′H-5,5′-bitetrazole-1,1′-diol) were selected for assembly with TNPDO. Thus, five assembled energetic materials, TNPDO-ADNP (**1**), TNPDO-DNBT (**2**), TNPDO-55BT (**3**), TNPDO-DNABO (**4**), and TNPDO-BTO (**5**), were developed (Scheme 1).

Characterization results confirmed that all of them are insensitive, high-density energetic materials. In particular, the decomposition temperature of TNPDO-55BT (**3**) was higher than those of both of its precursors, and the density of TNPDO-DNABO (**4**) was ~1.96 g cm^{-3} with detonation velocity and pressure of 8895 m s^{-1} and 33.32 GPa, respectively, which were comparable with those of RDX (1.80 g cm^{-3}, 8867 m s^{-1}, 34.07 GPa) and higher than those of TNPDO-TNBI (1.89 g cm^{-3}, 8648 m s^{-1}, 33.17 GPa). Furthermore, TNPDO-55BT (**3**) and TNPDO-BTO (**5**) were synthesized in 30 seconds. Overall, this work not only realized a strategy for the preparation of low sensitive or insensitive high-energy materials through simple molecular self-assembly but also developed five promising insensitive, high-density energetic materials.

Results and discussion

Experimental section

TNPDO monohydrate (1 mmol) was mixed with water (50 mL) at 90 °C, and the corresponding acidic precursors (2 mmol, or 1 mmol) were mixed with water (15 mL) at 85 °C. After both components were completely dissolved, the solutions were mixed and stirred for 30 minutes. The mixture was cooled to room temperature. During the processes of mixing and cooling, tiny crystals formed in the TNPDO-ADNP (**1**), TNPDO-DNBT (**2**) and TNPDO-DNABO (**4**) mixing systems. After filtration, a crystal sample appeared in the filtrate in about 2 days. The crystals were then separated by filtration and washed with a small amount of water and dried for their characterizations.
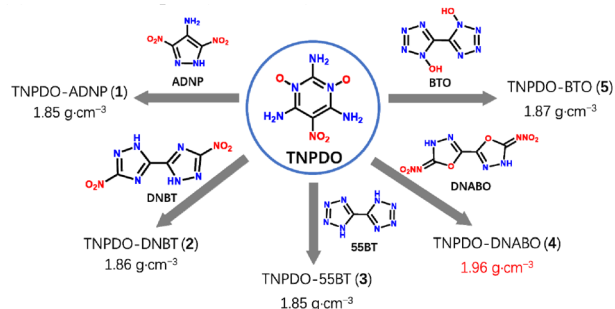
Crystal structures of TNPDO-ADNP (**1**), TNPDO-DNBT (**2**) and TNPDO-DNABO (**4**) were confirmed by single-crystal X-ray diffraction. TNPDO-55BT (**3**) and TNPDO-BTO (**5**) were fully characterized using NMR spectroscopy, IR spectroscopy, elemental analysis and powder XRD to determine their structure. More experimental details on the characterizations are shown in the ESI.†

Single crystal structures

TNPDO-ADNP (**1**) crystallized as a pentahydrate in the triclinic space group $P\bar{1}$ and contained two molecules per unit cell. The crystal density of **1** at 144 K is 1.735 g cm^{-3}, and its strong hydrogen bonds and packing structure are shown in Fig. 1a and b. In the **1** 5H$_2$O structure, ADNP and TNPDO are linked to each other *via* strong hydrogen bonds with water molecules, which are also linked *via* much stronger hydrogen bonds with bond lengths of 1.845 Å, 1.731 Å, 1.776 Å, and 1.707 Å, respectively (Fig. S14a†). As shown in Fig. 1a, in addition to the strong hydrogen bonding between ADNP, TNPDO and water molecules, there are also complex hydrogen bonding networks between ADNP and TNPDO molecules. The hydrogen bond lengths between ADNP and TNPDO are 2.141 Å and 2.180 Å, respectively. In addition, packing of ADNP and TNPDO form face-to-face π–π stacking with a layer spacing of 3.159 Å. Thus, strong hydrogen bonds and face-to-face π–π packing enhance its stability.[15,25–27] TNPDO-DNBT (**2**) belongs to the orthorhombic system and $Pna2_1$ space group. The crystal density of **2** at 173 K is 1.827 g cm^{-3}. Its strong hydrogen bonds and packing structure are shown in Fig. 1c and d. TNPDO and DNBT interact through a pair of hydrogen bonds in the structure of **2**·2H$_2$O, where a much stronger hydrogen bond is present with a bond length of 1.375 Å (Fig. S14c†). TNPDO and DNBT alternately form supramolecular structures through two pairs of hydrogen bonds, and the dislocation stacking increases their bulk density.[26] The crystal of TNPDO-DNABO (**4**) has two asymmetric units in the unit cell and exhibits a density of 1.859 g cm^{-3} at 100 K. Its strong hydrogen bonds and packing structure are shown in Fig. 1e and f. In the structure of **4**·5H$_2$O, TNPDO and DNABO in the same layer are connected by hydrogen bonds, while TNPDO in the two adjacent layers are connected by a much stronger hydrogen bond of bond length 1.318 Å (Fig. S14e†). This is possibly due to the rapid formation of TNPDO-
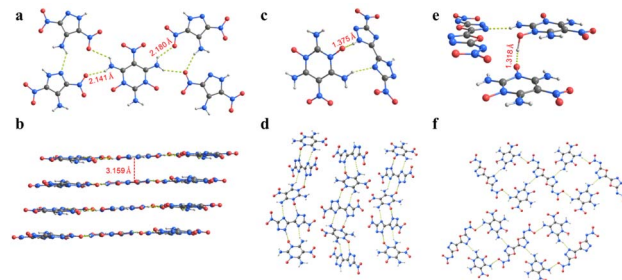

Scheme 1 Five assembled insensitive, high-density energetic materials based on TNPDO.

Fig. 1 (a) Hydrogen bonds in **1**. (b) Packing structure of **1**. (c) Hydrogen bonds in **2**. (d) Packing structure of **2**. (e) Hydrogen bonds in **4**. (f) Packing structure of **4**.

This journal is © The Royal Society of Chemistry 2025

J. Mater. Chem. A, 2025, **13**, 5164–5168 | **5165**

55BT (**3**) and TNPDO-BTO (**5**) (ESI†). However, their crystal morphology is not good enough to be determined *via* X-ray diffraction. Interestingly, there is no crystal water in the structures of **3** and **5**, which was proved *via* elemental analysis (Experimental section in the ESI†).

Sensitivity, density and thermostability

All crystal water molecules of **1**, **2** and **4** were removed prior to determining sensitivity, density and thermal stability. The measurements of impact and friction sensitivities show that all the resultant assembled materials are close to or equal to that of the less sensitive precursor resulting from the compromised or lower ESP (electrostatic potential) compared to precursors (Fig. S15 and Table S3†).[28] They were much more stable (impact and friction) than RDX and HMX and even better than TNT, except for TATB.[10,15] It was seen from Table 1 that **1–5** (>40 J, >360 N) are insensitive high-energy materials, which resulted from the intramolecular hydrogen bonds of TNPDO and the hydrogen bond (HB) network between TNPDO and acidic high-energy molecules. For most salts or co-crystals, their density is usually lower than that of their precursors. Generally, introducing ions or molecules would change the original stacking mode and interlayer spacing of the parent molecule, resulting in a decrease in its density. However, TNPDO-55BT (**3**) (1.85 g cm^{-3}) had an equal or higher density than either of its precursors (TNPDO: 1.85 g cm^{-3}; 55BT: 1.70 g cm^{-3}) (Table S4†). The higher density was owing to the removal of the crystal H$_2$O and closer packing coefficients caused by short HBs in the resulting crystals. Notably, the density of TNPDO-BTO (**5**) (1.87 g cm^{-3}) was even larger than those of either of the dehydrated precursors (TNPDO: 1.85 g cm^{-3} and BTO: 1.82 g cm^{-3}). This indicates that compound **5** may have a closer packing mode and stronger hydrogen bonds between TNPDO and BTO. The density of TNPDO-DNABO (**4**) was 1.96 g cm^{-3}, which was slightly lower than that of DNABO (1.99 g cm^{-3}).
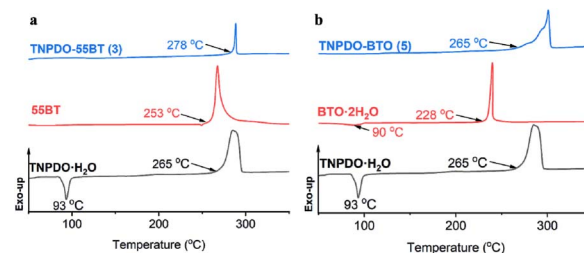

Fig. 2 . DSC curves of TNPDO-55BT (**3**) (a), TNPDO-BTO (**5**) (b) and their precursors.

Differential scanning calorimetry (DSC) measurements were performed to determine the thermal stability of dried **1–5** at a heating rate of 5 °C min^{-1} (Fig. 2 and S16†). The decomposition temperatures of the five compounds **1–5** were 186, 185, 278, 185, and 265 °C, respectively. TNPDO-BTO (**5**) also exhibited an equal or higher decomposition temperature than either of its precursors (TNPDO: 265 °C and BTO: 228 °C). Compared to precursors of TNPDO-BTO (**5**), TNPDO·H$_2$O had an endothermic peak at around 93 °C and BTO·2H$_2$O had a similar peak at around 90 °C, which are losing crystal water temperatures. TNPDO-BTO (**5**) had no endothermic peak, indicating that it did not contain crystal water (Fig. 2b). Interestingly, the decomposition temperature of **3** (278 °C) was also higher than either of its dehydrated precursors (TNPDO: 265 °C and 55BT: 253 °C) (Fig. 2a). The high densities and thermal stabilities of compounds **3** and **5** indicate that their molecular packing is tighter and hydrogen bonding is stronger than their precursors. These results show that these compounds not only have a high density but also possess acceptable safety properties.

Theoretical analysis

Determining the significantly different stabilities of compounds based on TNPDO was essential. Hirshfeld surface analysis

Table 1 Physical properties of assembled energetic materials

Compound	T_d [a] (°C)	ρ [b] (g cm^{-3})	$\Delta_f H$ [c] (kJ mol^{-1})	D_v [d] (m s^{-1})	P [e] (GPa)	IS [f] (J)	FS [g] (N)
TNPDO-ADNP (**1**)	186	1.85	100	8434	28.92	>40	>360
TNPDO-DNBT (**2**)	185	1.86	304	8376	28.28	>40	>360
TNPDO-55BT (**3**)	278	1.85	540	8565	27.80	>40	>360
TNPDO-DNABO (**4**)	185	1.96	204	8895	33.32	>40	>360
TNPDO-BTO (**5**)	265	1.87	579	8715	30.33	>40	>360
TNPDO-TNBI[h]	275	1.89	237.5	8648	33.17	43	>360
ADNP	175	1.90	96	8770	33.21	>40	>360
DNBT	256	1.86	285	8434	29.29	10	360
55BT	253	1.70	570	8191	24.27	10	144
DNABO	187	1.99	167	9231	37.55	5	60
BTO	228	1.82	595	9181	34.95	7	120
TNPDO	265	1.85	−8	8356	27.17	>40	>360
TNT[i]	295	1.65	−60	6840[j]	18.56[j]	15	350
TATB[k]	315	1.94	−154	8265[j]	28.00[j]	50	>360
RDX[k]	205	1.80	70	8867[j]	34.07[j]	7.5	120
HMX[k]	270	1.91	75	9261[j]	38.21[j]	7.5	120

[a] Decomposition temperature (onset). [b] Experimental density at room temperature. [c] Heat of formation. [d] Detonation velocity. [e] Detonation pressure. [f] Impact sensitivity. [g] Friction sensitivity. [h] Ref. 27. [i] Ref. 10. [j] Data were provided by EXPLO 5 (6.07 version). [k] Ref. 15.
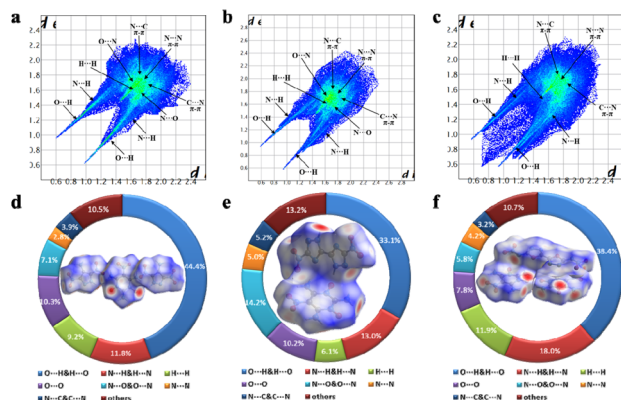
Fig. 3 2D fingerprint plots of **1**, **2**, and **4** (a–d) and Hirshfeld surfaces and percentage contributions of individual atomic contacts for **1**, **2**, and **4** (e–f).

serves as an insightful approach to elucidate the intricacies of intermolecular interactions.[29,30] This includes comprehensive intermolecular interactions, such as hydrogen bonds, halogen bonds, π-stacking, and lone pair-π (π–π) interactions, as well as the intricate patterns of molecular stacking.[31] Thus, this methodological revelation would not only enhance our understanding of the structural nuances of the compounds but also paves the way for designing energetic materials with tailored properties. Hirshfeld surface analysis and two-dimensional (2D) fingerprint plots for compounds **1**, **2**, and **4** are depicted in Fig. 3. In these co-crystalline structures, the N···H and O···H interactions and percentage contributions of individual atomic contacts for **1**, **2**, and **4** (e and f) are prominently featured, constituting a significant proportion of 56.2%, 46.1%, and 56.4%, respectively. These interactions play an important role in their thermal stabilities. Although the crystal morphology of **3** and **5** was not good, their extremely fast reaction rate in the aqueous solution (ESI†) prove that the two precursors form a strong hydrogen bond among themselves, and therefore, they have equal or higher stability than their precursors. Further, noncovalent interaction calculations (NCI) were used to analyze the effects of hydrogen bonds on stabilities of **1**, **2** and **4** (Fig. 4).[27,32] The NCI calculation results showed that there are a large number of hydrogen bond interactions in **1**, **2** and **4**. The presence of these hydrogen bonds contribute to the satisfactory stabilities of **1**, **2** and **4**.
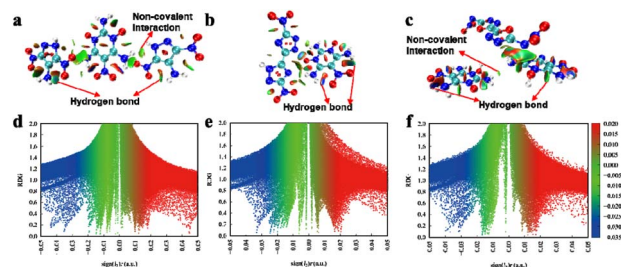

Fig. 4 Noncovalent interaction plots of gradient isosurfaces of **1** (a and d), **2** (b and e), and **4** (c and f).

Energy properties

The heat of formation (HOF) of a compound is a necessary parameter to calculate its detonation performance. Hence, the HOFs of the resulting energetic compounds were calculated using a simple and updated method (see ESI†). Since these five assembled materials are composed of two high-energy materials, all of them exhibit high positive HOF values (>100 kJ mol^{-1}). From the observed experimental densities, the detonation performances were calculated using the professional software EXPLO5 6.07 (Table 1).[33] Notably, the detonation performances of all assembled materials exceeded that of TNT and were better than that of TATB. Among them, the detonation performances of TNPDO-DNABO (**4**) (8895 m s^{-1}, 33.32 GPa) were comparable to those of RDX (8867 m s^{-1}, 34.07 GPa), especially its high density and positive HOF. Interestingly, the detonation properties of TNPDO-55BT (**3**) (8565 m s^{-1}, 27.80 GPa) were higher than those of either of their corresponding anhydrous precursors (TNPDO: 8356 m s^{-1}, 27.17 GPa; 55BT: 8191 m s^{-1}, 24.27 GPa). This resulted from the synergistic effects of density, HOF and oxygen balance of the resultant crystals compared to their precursors. Thus, these materials demonstrated their potential as excellent energetic materials.

Conclusions

In this work, we combined TNPDO with five distinct acidic energetic compounds and successfully synthesized five high-density energetic materials through a hydrogen bonding self-assembly approach. All resultant assembled materials exhibited commendable thermal stability (>185 °C) and insensitivity to mechanical stimuli (>40 J, >360 N). TNPDO-55BT (**3**) and TNPDO-BTO (**5**) exhibited equal or higher decomposition temperatures than either of their precursors. Moreover, the majority of these materials demonstrated superior detonation performance, resulting from the synergistic effects of density, heat of formation (HOF), and oxygen balance. Notably, the detonation properties of **3** (8565 m s^{-1}, 27.80 GPa) are higher than those of either of their corresponding anhydrous precursors (TNPDO: 8356 m s^{-1}, 27.17 GPa; 55BT: 8191 m s^{-1}, 24.27 GPa). The density of TNPDO-DNABO (**4**) was 1.96 g cm^{-3} with detonation performances of 8895 m s^{-1} and 33.32 GPa, which were comparable to those of RDX (8867 m s^{-1}, 34.07 GPa). TNPDO-BTO (**5**) exhibited a higher density than its dehydrated precursors, further enhancing their energetic characteristics. In summary, simple preparation procedure, insensitivity, acceptable thermal stability and excellent detonation properties make these five resultant materials promising high-energy materials. Furthermore, this work may pave the way to simple preparation strategies for low sensitive or insensitive high-energy materials.

Data availability

All data relevant to the work described here are available in the ESI† or from the CCDC.

This journal is © The Royal Society of Chemistry 2025

J. Mater. Chem. A, 2025, **13**, 5164–5168 | **5167**

Author contributions

Jichuan Zhang, Jiaheng Zhang and Jean'ne M. Shreeve designed the study. Jichuan Zhang performed most of the experiments and measurements. Jinhao Zhang completed the theoretical calculations. Richard J. Staples performed crystallographic structural analysis. Jinhao Zhang, Jichuan Zhang, Jiaheng Zhang, and Jean'ne M. Shreeve prepared the manuscript.

Conflicts of interest

There are no conflicts to declare.

Acknowledgements

References

1 J. Zhang, L. A. Mitchell, D. A. Parrish and J. M. Shreeve, *J. Am. Chem. Soc.*, 2015, **137**(33), 10532–10535.

2 J. Zhang, J. Zhang, D. A. Parrish and J. M. Shreeve, *J. Mater. Chem. A*, 2018, **6**(45), 22705–22712.

3 Y. Song, Q. Huang, J. Zhang, Y. Zhang, B. Jin and R. Peng, *Propell. Explos. Pyrot.*, 2022, **47**(9), 1–10.

4 V. M. Boddu, D. S. Viswanath, T. K. Ghosh and R. Damavarapu, *J. Hazard. Mater.*, 2010, **181**(1–3), 1–8.

5 T. M. Klapötke, C. Petermayer, D. G. Piercey and J. Stierstorfer, *J. Am. Chem. Soc.*, 2012, **134**(51), 20827–20836.

6 D. Fischer, T. M. Klapötke and J. Stierstorfer, *Angew. Chem., Int. Ed.*, 2015, **54**(35), 10299–10302.

7 C. Zhang, C. Sun, B. Hu, C. Yu and M. Lu, *Science*, 2017, **355**, 374–376.

8 M. Deng, Y. Feng, W. Zhang, X. Qi and Q. Zhang, *Nat. Commun.*, 2019, **10**(1), 1339–1346.

9 T. E. Khoranyan, A. A. Larin, K. Y. Suponitsky, I. V. Ananyev, I. N. Melnikov, E. K. Kosareva, N. V. Muravyev, I. L. Dalinger, A. N. Pivkina and L. L. Fershtat, *ACS Appl. Mater. Interfaces*, 2024, **16**, 53972–53979.

10 J. Ma, J. Tang, H. Yang, H. Yi, G. Wu, S. Zhu, W. Zhang, Y. Li and G. Cheng, *ACS Appl. Mater. Interfaces*, 2019, **11**, 26053–26059.

11 J. C. Bennion and A. J. Matzger, *Acc. Chem. Res.*, 2021, **54**, 1699–1710.

12 N. Fischer, D. Fischer, T. M. Klapötke, D. G. Piercey and J. Stierstorfer, 2012, *J. Mater. Chem.*, **22**, 20418–20422.

13 N. Fischer, T. M. Klapötke, M. Reymann and J. Stierstorfer, *Eur. J. Inorg. Chem.*, 2013, **2013**(12), 2167–2180.

14 J. Zhang, B. Jin, R. Peng, C. Niu, L. Xiao, Z. Guo and Q. Zhang, *Dalton Trans.*, 2019, **48**(31), 11848–11854.

15 J. Zhang, Z. Jin, W. Hao, Z. Guo, Y. Wang, R. Peng and B. Jin, *Cryst. Growth Des.*, 2023, **23**(6), 4499–4505.

16 J. F. Remenar, S. L. Morissette, M. L. Peterson, B. Moulton, J. M. MacPhee, H. R. Guzmán and Ö. Almarsson, *J. Am. Chem. Soc.*, 2003, **125**, 8456–8457.

17 Q. Lai, L. Pei, T. Fei, P. Yin, S. Pang and J. M. Shreeve, *Nat. Commun.*, 2022, **13**(1), 6937–6946.

18 A. J. Bennett, L. M. Foroughi and A. J. Matzger, *J. Am. Chem. Soc.*, 2024, **146**(3), 1771–1775.

19 Q. Lai, Y. Long, P. Yin, J. M. Shreeve and S. Pang, *Acc. Chem. Res.*, 2024, **57**(19), 2790–2803.

20 Q. Yin, P. Zhao, R. J. Sa, G. C. Chen, J. Lu, T. F. Liu and R. Cao, *Angew. Chem., Int. Ed.*, 2018, **57**(26), 7691–7696.

21 J. Zhang, Y. Feng, R. J. Staples, J. Zhang and J. M. Shreeve, *Nat. Commun.*, 2021, **12**(1), 2146–2152.

22 J. Zhang, Y. Feng, Y. Bo, A. K. Chinnam, J. Singh, R. J. Staples, X. He, K. Wang, J. Zhang and J. M. Shreeve, *Chem*, 2022, **8**(10), 2678–2687.

23 Y. Wang, Y. Liu, S. Song, Z. Yang, X. Qi, K. Wang, Y. Liu, Q. Zhang and Y. Tian, *Nat. Commun.*, 2018, **9**(1), 2444–2454.

24 J. Zhang, Y. Feng, Y. Bo, R. J. Staples, J. Zhang and J. M. Shreeve, *J. Am. Chem. Soc.*, 2021, **143**(32), 12665–12674.

25 C. Zhang, X. Wang and H. Huang, *J. Am. Chem. Soc.*, 2008, **130**, 8359–8365.

26 Y. Hu, W. S. Dong, Z. J. Lu, H. Zhang and J. G. Zhang, *Chem. Commun.*, 2023, **59**(65), 9864–9867.

27 J. Zhang, J. Zhang, J. Singh, W. Wu, R. J. Staples, J. Zhang and J. M. Shreeve, *J. Mater. Chem. A*, 2024, **12**(10), 5918–5923.

28 J. S. Murray and P. Politzer, *Wiley Interdiscip. Rev.: Comput. Mol. Sci.*, 2011, **1**(2), 153–163.

29 S. Li, R. Bu, R.-j. Gou and C. Zhang, *Cryst. Growth Des.*, 2021, **21**(12), 6619–6634.

30 J. Zhang, Z. Guo, Y. Song, W. Hao, R. Peng and B. Jin, *Chem. Eng. J.*, 2023, **453**, 139762–139767.

31 C. Lei, C. Xiao, J. Tang, H. Yang, Q. Zhang and G. Cheng, *Chem. Commun.*, 2023, **59**(76), 11389–11392.

32 F. Yang, Y. Xu, P. Wang, Q. Lin and M. Lu, *Cryst. Growth Des.*, 2021, **22**(1), 167–173.

33 M. Sućeska, *EXPLO5, Ver. 6.07*; Brodarski Institute: Zagreb, Croatia, 2013.

5168 | *J. Mater. Chem. A*, 2025, **13**, 5164–5168

This journal is © The Royal Society of Chemistry 2025